Lorenzo Brezzi · Alberto Bisson · Davide Pasa · Simonetta Cola

Innovative passive reinforcements for the gradual stabilization of a landslide according with the observational method

Abstract A large number of landslides occur in North-Eastern Italy during every rainy period due to the particular hydrogeological conditions of this area. Even if there are no casualties, the economic losses are often significant, and municipalities frequently do not have sufficient financial resources to repair the damage and stabilize all the unstable slopes. In this regard, the research for more economically sustainable solutions is a crucial challenge. Floating composite anchors are an innovative and low-cost technique set up for slope stabilization: it consists in the use of passive sub-horizontal reinforcements, obtained by coupling a traditional self-drilling bar with some tendons cemented inside it. This work concerns the application of this technique according to the observational method described within the Italian and European technical codes and mainly recommended for the design of geotechnical works, especially when performed in highly uncertain site conditions. The observational method prescribes designing an intervention and, at the same time, using a monitoring system in order to correct and adapt the project during realization of the works on the basis of new data acquired while on site. The case study is the landslide of Cischele, a medium landslide which occurred in 2010 after an exceptional heavy rainy period. In 2015, some floating composite anchors were installed to slow down the movement, even if, due to a limited budget, they were not enough to ensure the complete stabilization of the slope. Thanks to a monitoring system installed in the meantime, it is now possible to have a comparison between the site conditions before and after the intervention. This allows the evaluation of benefits achieved with the reinforcements and, at the same time, the assessment of additional improvements. Two stabilization scenarios are studied through an FE model: the first includes the stabilization system built in 2015, while the second evaluates a new solution proposed to further increase the slope stability.

Keywords Landslide stabilization · Observational method · Passive reinforcement · Floating anchor · Composite bar · Slope stability

Introduction

In the areas where very exceptional rainy events have caused the contemporaneous triggering of a large number of slope instabilities, the administration working for soil protection has to face a difficult challenge. On one hand, they need to restore the safety conditions in as many landslides as possible in the shortest time possible. On the other hand, they often do not have sufficient economic means to restore all the situations. In this condition, the challenge is the selection of interventions that offer the lowest cost-benefit ratios in relation to the nature and kinematics of the instability, engineering and economic feasibility, and social and environmental acceptability (Popescu 2001; 2002; Popescu and Seve 2001; Galve et al. 2016; Kazmi et al. 2017). Other important features must be the rapidity of installation and the possibility of being modulated over time. Modularity is a factor which is not always considered, but is very important because it allows the works to be carried out in various steps: firstly, the interventions needed to slow down the movements and, subsequently, after the acquisition of a deeper knowledge of the site conditions, the interventions that guarantee higher safety conditions in relation to legal requirements.

On the other hand, efficiency is evaluated as the increment of slope stability conditions, determined by stability analyses. Independently from the method adopted for the stability analysis, i.e., a method based on limit equilibrium approach (Morgenstern 1992; Abramson et al. 2002) or a finite element method (Ugai and Leshchinsky 1995; Dawson et al. 1999; Griffiths and Lane 1999; Cheng et al. 2007; Gao et al. 2013) or others, stability analyses give reliable results only if a comprehensive knowledge of the slope is available (Baecher and Christian 2008; Hong and Roh 2008; Hicks and Spencer 2010; Stark and Hussain 2012; Ji et al. 2018). However, when engineers have to operate in an emergency, they have little available information about the geometry, the landslide kinematics, and the properties of the soils involved. Consequently, they are induced to overestimate the interventions required for stabilization with an increment of costs and a reduction of the number of instabilities that can be recovered. Moreover, even when one can perform some investigations before designing the remedial works, site characterization always presents a level of uncertainty due to the natural heterogeneity of the slopes.

In all these cases, when the prediction of geotechnical behavior is difficult, it may be appropriate to use the approach called "Observational Method" (Eurocode 7 2004; Calvello 2017; NTC 2018). The observational method is a framework wherein construction and design procedures and details of a geotechnical engineering project are adjusted based upon observations and measurements made as construction proceeds (Peck 1969). Of course, specifically citing Eurocode 7 (2004), when the observational method is adopted "acceptable limits of behaviour shall be established, the range of possible behaviour shall be assessed and it shall be shown that there is an acceptable probability that the actual behaviour will be within the acceptable limits." Then, "a plan of monitoring shall be devised, which will reveal whether the actual behaviour lies within the acceptable limits" and "the response time of the instruments… shall be sufficiently rapid in relation to the possible evolution of the system." This means that, independently from the geotechnical problem at hand, an effective application of the observational method requires firstly a properly planned monitoring strategy, comprising an appropriate choice of variables to monitor, the set-up of a reliable monitoring system

and the choice of criteria to evaluate the monitoring results. Secondly, it needs a real-time analysis of the observations and the planning of alternative construction strategies to be adopted depending on the results of the data analysis (Calvello 2017).

This approach is easily adoptable in all the projects in which an appropriate variable to monitor and its threshold value can be easily identified, such as in the construction of embankment or the realization of an underground excavation. On the contrary, the application of the observational method to landslides requires a change of approach, if the designer wants to verify the effectiveness of the intervention during the works or immediately after. In fact, a slope interested by a landslide often moves slowly before the collapse occurs, it evidences great displacement rate during and after the collapse, and, moreover, its rate is strongly influenced by exceptional meteoric conditions. Finally, the reduction of this rate to a negligible value is generally a difficult goal to pursue because it requires high economic investments. Hence, the application of the method can be carried out by defining a maximum displacement rate threshold in relation to the required level of stability, i.e., in relation to the safety degree to be guaranteed. Made this choice, the design of remedial works is finalized at reaching this condition. Then, the monitoring performed during and after the work allows to verify the effectiveness of the intervention compared to expectations and, if necessary, to adapt the chosen solution. In this regard, once again, a modular technique offers the advantage of being adapted during its installation on site in relation to the results of monitoring and data analysis.

In this context, in recent years, many efforts have focused on the study of a new slope reinforcement system, namely that of *passive composite floating anchors* (Bisson and Cola 2014; Bisson 2015; Bisson et al. 2015, 2016, 2018; Cola et al. 2019), which, at the same time, enables costs to be greatly reduced respect other reinforcement techniques and the modular criteria to be respected (Bisson and Cola 2014). In their work, Bisson and Cola (2014) compared seven different slope stabilization techniques, i.e., cantilever walls, gabion walls, single bored piles, micropiles-based walls, anchored sheet-piles walls, and, indeed, soil nailing, choosing a common slope geometry to be used to estimate costs and effects on the slope stability of each solution. The analyses pointed out that the most advantageous solution in terms of ratio between intervention cost and slope safety factor increase is precisely that obtained with passive anchors.

In order to explain how this new system works and can be managed in accordance with the observational method, after a brief presentation of the new technique and its advantages, this paper deals with its application for the stabilization of a real landslide.

Composite anchors

Slope stabilization with reinforcements is a common practice that aims to increase shear strength and/or reduce the sliding actions along the slip surface with many different types of structures. Retaining walls, dowels or structural wells, micropile systems or reticulates, tied-back micropile sheet-walls, active anchors, and soil nailing are all systems used in medium deep landslides, i.e., when the sliding involves masses up to medium depths (8–16 m). Even if out of all of them, soil nailing is the most recent proposal

in chronological order because it was developed relatively late (Stocker 1976; Gassler and Gudehus 1981), it offers several advantages compared with other systems. The bars used for soil nailing are installed in the soil with small and flexible boring machines and with minimal soil excavation. They act as passive anchors without pre-tension in the installation phase: consequently, their installation is very rapid, and they do not require control over time. They can be installed in all types of soils and rocks and their length and orientation can be adapted to almost all surficial and deep morphologies, based on the in situ observation performed before and during installation. Finally, comparisons with other reinforcement methods have shown that soil nailing is generally more economical than other techniques (Ansari and Domitric 1992; FHWA 2003; Bisson and Cola 2014).

Thanks to its advantages, nowadays, soil nailing is a common practice for the support of excavations and specific guidelines are available in many countries (e.g., Geoguide7 2008; EN 14490:2010 2010). On the contrary, its application to the stabilization of natural unstable slopes advances more slowly, even if many works that explain soil nailing effects on landslides have already been published (Turner and Jensen 2005; Ng et al. 2007; Pun and Urciuoli 2008; Bisson et al. 2015; Sharma et al. 2019; Cola et al. 2019).

The *composite anchor* is an advancement of the traditional self-drilling bar used for soil nailing, developed by an Italian company with the aim of improving the mechanical resistance of the standard soil nailing bars and expanding their applications, especially in the field of landslide stabilization (Bisson 2015; Bisson et al. 2015; 2018; Cola et al. 2019).

A composite anchor consists of a traditional carbon steel self-drilling bar with one or more harmonic steel tendons inserted and cemented inside the central cavity of the bar. The system is completed by an external plate for locking the bar and a protective cover for the tendon head (Fig. 1).

The installation of these anchors develops in the following steps:

A. Installation of the self-drilling bar up to the design depth, eventually adapting the overall length to the position of the resistant deep layer.
B. Manual insertion of one or more harmonic steel tendons in the central cavity of the bar before the inner grout hardens.
C. Application and connection of the external plate, which has the role of contrasting the movement of the external soil surface.

When realized in this way, the anchors behave like passive elements. A possible variation in the installation procedure, specifically in step B, permits the anchor to become an active reinforcement. In this version, the most external portion of the cavity is washed by injection of water, thus obtaining the result that the anchors are divided into two parts: the foundation length, where the tendons are linked to the bar, and the most external part where the tendons are free. After the hardening of the grout in foundation, the strands can be tensioned and connected to the external plate by a special locking head. In this way, the tendons transmit an axial compression to the bar and the soil in depth, thus immediately increasing the stabilizing force along the sliding surface (Bisson et al. 2016).
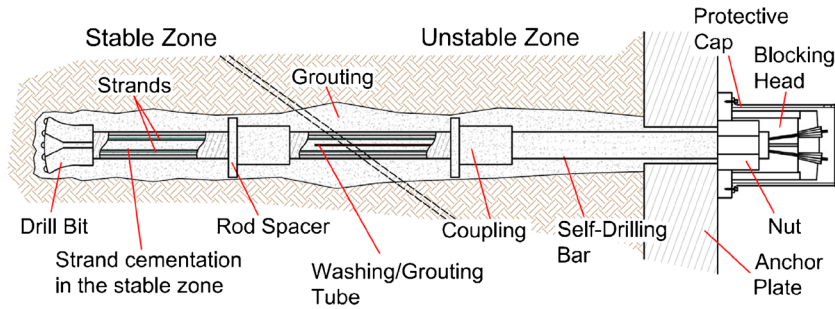
Fig. 1 Scheme of a composite anchor

Compared to traditional anchors and soil nailing bars, composite anchors offer additional advantages:

- possibility of selecting the length of each anchor in situ, thus adapting it to different geological and geotechnical conditions observed during the installation;
- lower cost with the same mechanical properties, because the harmonic steel of tendons has a lower price than the steel constituting the bar. By inserting the tendons, an increase of the overall resistant steel cross-section can be obtained, with a minor cost respect by using a larger cross-section of the hosting bar;
- greater flexural inertia and good continuity given by the inner strands;
- higher ultimate tensile forces since the composite anchors can reach up to 5000 kN that is more than 3 times the maximum ultimate tension of soil nailing bars;
- better durability (minor cracking, better protection from corrosion);
- easier transport, because the various constitutive elements can be transported separately, and easier installation, because all the advantages of the self-drilling technique are maintained.

Composite anchors can be used in consolidation of soil and rock cut slopes, in foundation reinforcements, and in landslide stabilization too. Particularly, in the slow-moving landslide and when the works must to be carried out in various steps, as described in the "Introduction" section, the anchors can be used in a *floating* configuration, as described in the next section.

Composite anchors in slow-moving landslide stabilization

The *floating* technique (Bisson et al. 2015, 2018) consists of installing passive sub-horizontal reinforcements, with a sufficient foundation in the bedrock, and coupled with individual external concrete slabs.

The most important feature is that the slabs, having appropriate shape and size, are not connected to each other, as depicted in Fig. 2, condition for which the anchors are defined as *floating*. If some slope movements occur, axial forces in the passive reinforcements develop because of the shear stresses transmitted by the slow-moving mass at the bars along the soil-grout interface: these axial forces contrast part of the forces inducing instability and can reduce the landslide evolution process until it completely stops. Since the axial head force at the connection with an external slab is small, the system does not require a continuous facing or strong and invasive external structures, and, when the slope deforms, the slabs may also be embedded inside the soil.

Since, for these applications, large installation depths (up to 55 m) and huge axial forces may be required, composite anchors are particularly suitable because they assure very high forces not achievable with standard soil nailing bars. As already mentioned, a pre-tension can be also assigned to the tendons with the aim of pre-activating the shear stress at the anchor-soil interface, thus reducing the relative displacements necessary for the complete development of the anchor resistance. If the pre-tension remains very small (1/10–1/8 of the working load of the anchor), this configuration can be defined as partially active.

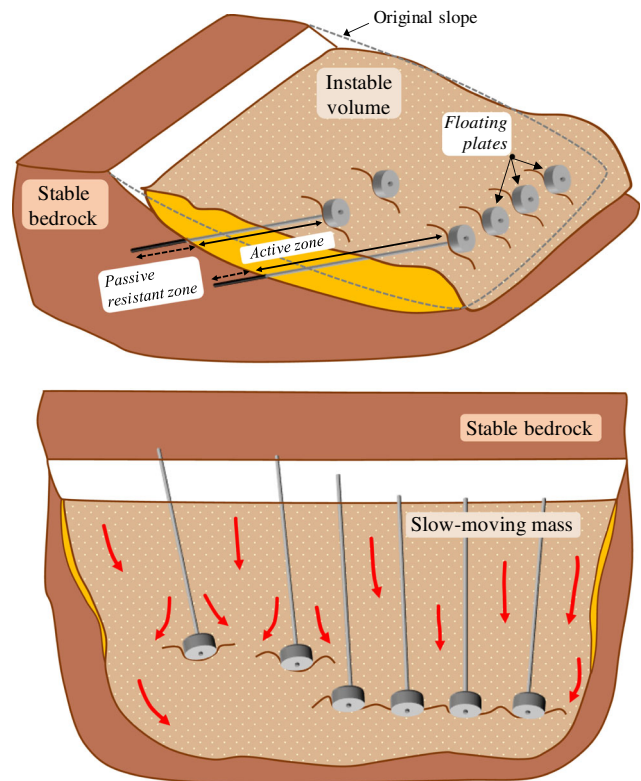**Fig. 2** Working scheme of the "floating anchor" technique with composite bars and external slab

As in soil nailing, the design capacity of a floating anchor depends on the available frictional strength at the soil-grout interface, as well as the size and the tensile strength of the bar itself. Therefore, it has to ensure that:

A. The tensile strength of the steel bars is sufficient to withstand the maximum developed axial stress; the total stabilizing force Q_a generated by each element is the sum of the head force absorbed by the floating plate Q_p and the integral of the friction stresses activated along the soil-grout interface in the active zone of the slope:

$$Q_a = Q_p + \int_0^{L_a} \pi D \cdot \tau_u(x) dx \qquad (1)$$

where D is the effective diameter of the anchor (bar with the cement grout around), L_a the length of the anchor in the active zone, and $\tau_u(x)$ the shear strength at the soil-grout interface at the coordinate x. The calculation of $\tau_u(x)$ can be performed by extending the methods proposed by Bustamante and Doix (1985) for micropiles or in accordance with the indications reported by FWHA (2003) or Hong Kong guidelines (Geoguide7 2008) or in some papers (Heymann et al. 1992; Yin et al. 2009).

B. The length of each bar within the passive zone, that is, the portion of the bars that extends beyond the potential or actual slip surface, is sufficient to provide a pull-out resistance equal to the total stabilizing force Q_a generated in the bar (Geoguide7 2008).

Due to the use of the floating elements, one of the most important advantages is that, if the slope movements do not completely arrest with the installation of these anchors, the soil can slide along the bars and the floating elements which remain embedded in the slope. In this way, the bars can find a new equilibrium condition without cracks or structural failure and without losing their effectiveness, unlike traditional rigid works, such as gravity or micropile walls. This behavior allows a progressive adapting of the intervention according to the observational method: if a first installation is not enough to stop the slope, i.e., the recorded moving rate does not decrease below a required limit, the intervention can subsequently be improved by adding other reinforcements.

The case study of Cischele landslide, illustrated in as follows, is used here to explain with an example this method of installing the composite anchors and how the intervention in this site was modulated with time according with the limited financial means of the local administration.

Cischele landslide

In November 2010, an exceptional rainfall (817 mm in less than 3 days) affected the North-Eastern of Italy and, in particular, the Vicenza Province, activating several slope instabilities (Floris et al. 2013): in particular, more than 500 new landslides were reported in the mountain area of the Province. Among these, in Cischele, a small hamlet in the territory of Recoaro Terme, the activation of movements in an area of about 16,000 m² was observed. The unstable area is approximately 120 m wide and 180 m long (Fig. 3), is located at an altitude between 550 m and 600 m a.s.l., and presents a mean inclination of 24°. The instability affected and damaged some houses and the main road crossing the hamlet (Fig. 4). Several fractures appeared during the rainy event and have been gradually increasing thereafter, associated with continued subsidence of roads and pavements in the private car parking, all at the continuous develop evidence of sliding movements in the following months.

As the administration had very limited financial means and could not carry out immediately all the works indicated as necessary for the complete stabilization of the area, it was decided to carry out an intervention subdivided in two phases and apply the observational approach to control the improvement induced by each step. In this way, after a first phase of monitoring the movements, necessary to individuate the landslide geometry, a partial stabilization was carried out with the installation of a series of passive anchors. The monitoring continued in the post-installation phase in order to collect data for an evaluation of the improvements obtained. Furthermore, the site was studied using an FE model which was calibrated on the pre-intervention and post-intervention conditions in order to investigate the level of further improvement achievable if the planned stabilization works could be completed.

Geology

The slope is based on the crystalline basement of the Recoaro subalpine area consisting of quartz-Phyllite, a high strength metamorphic schistose rock. Above this stratum, a sedimentary rock composed of clastic deposits, such as quartz and feldspars sands and silts, locally known as Val Gardena Sandstone, is present. At the top, there is the Bellerophon formation, another sedimentary rock consisting mainly of limestone, often minutely decayed, with frequent interbedded silty clays in the lower part. A major tectonic action affects the area, due to the compression time of the Alpine orogeny. This makes the Schists crystalline basement visible in some places on the surface. The unstable area is located between two major vertical faults with a prevailing backing horizontal movement.

In order to better characterize the stratigraphic profile of the area, several continuous core surveys were carried out. In particular (Fig. 3):

- Three surveys in 2011 (S1, S2, S3), (green circles);
- Two surveys in 2012 (S4, S5), (red circles);
- Four surveys in 2014 (A, B, C, D), (blue circles).

In the central part of the slope, a 10–12-m thick cover, consisting of completely weathered Bellerophon Limestone, lies above a clayey silt and sandy clay layer originating from an alteration of Val Gardena Sandstone. Up to a depth of 20–30 m from the ground surface, a bedrock of low to medium-altered Phyllites was found. At the landslide toe, below the first 5 m of
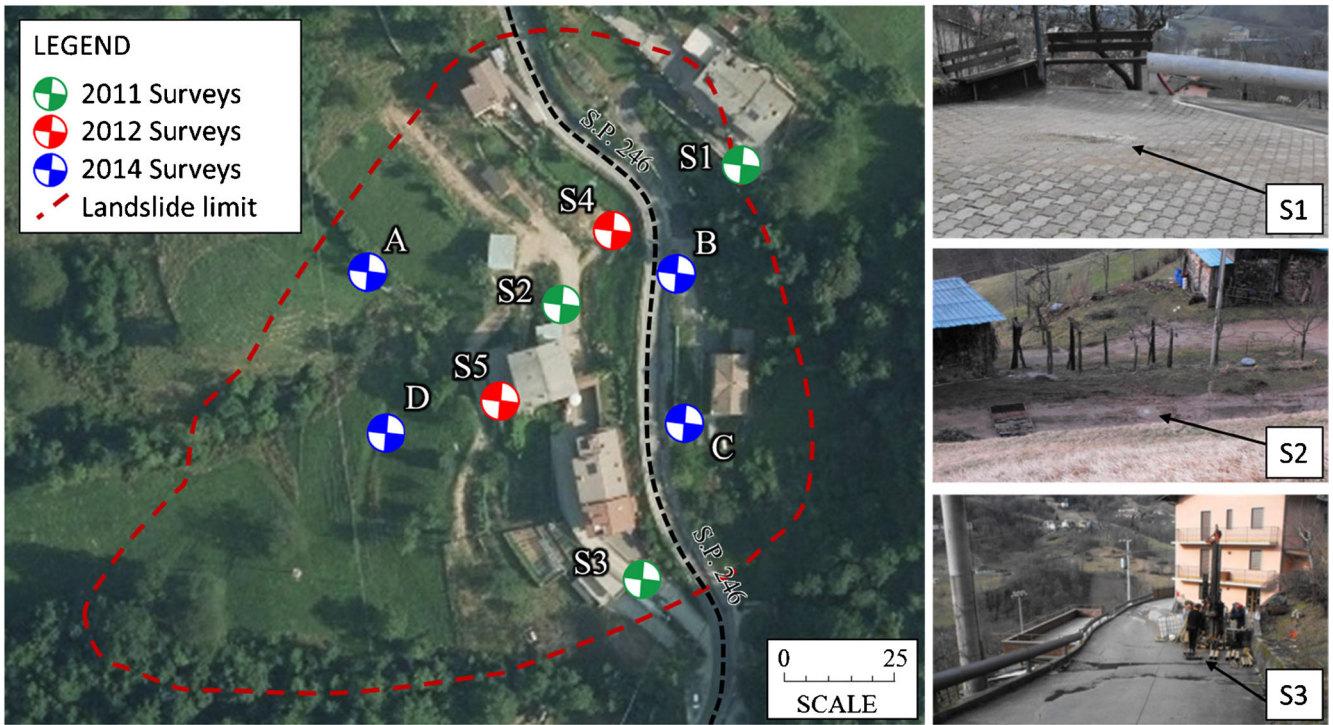
Fig. 3 Cischele landslide orthophoto, with indication of in situ borehole's locations and the landslide limits

backfill clay, a strongly altered Phyllite in a reddish silty clay matrix exists, but Sandstone or Bellerophon layers are not noticed.

In addition to these stratigraphic units, a thin silty sandy clay interface between limestones and sandstones was identified. This layer, having a thickness of 30–70 cm, was observed in boreholes S2, A, and B in the central portion of the landslide area, at a depth ranging from 12 to 18 m. It has reduced mechanical characteristics compared to neighboring materials and it could represent the layer in which the likely sliding surface of the landslide is located.

Soil characterization

Considering the complex geology of the area, further geotechnical tests were carried out. In particular, three in situ permeability tests and four standard penetrometric tests (SPT) were performed during borehole execution. Several grain-size analysis and determination of Atterberg limits and shear friction angles of different soil samples were also executed. The internal friction angle values, obtained from the shear tests on some siltstone and sandstone samples collected at depths between 11 and 18.50 m from the layer

Fig. 4 Some damages caused by the Cischele landslides on: (**a**) the main road; (**b**) a house

above the Phyllites, were taken into consideration. The friction angle values of the shallower soils were instead obtained by the SPT carried out on the upper layers inside the first probing hole. A summary of the soil properties is reported in Table 1.

Note that the interface is considered mainly composed of degraded Val Gardena sandstone, so its friction angle value is assumed a little bit lower than that of the intact soil. A null cohesion is then assumed, considering the material localized along the sliding surface having reached the residual resistance.

The observational method on the realized stabilization works

Pre-intervention situation

In order to monitor the movement of the landslide body over time, to allow the planning of the interventions that had to be carried out on the slope, two inclinometers were inserted inside the S1 and S3 surveys. In the first months of 2011, three measurements were performed, approximately monthly. The inclinometer CK1, inserted in the S1 hole and located in a portion of relatively stable ground beyond the landslide crown, recorded minimal displacements, in the order of a few millimeters per year. The CK2 inclinometer, installed in S3 hole, allowed the measurement of non-negligible displacements (Fig. 5), even if not very large because of the brevity of the recording period: moreover, it showed a large increment (from 5 to 13 mm) in correspondence with the March rains (273 mm), confirming the strong correlation between the gravitational movements and the rain. The slip surface was pinpointed at the contact between the Bellerophon formation and the Val Gardena Sandstone. The slow progress of the landslide proceeded with an indicative speed of just over 40 mm/year.

Since the inclinometer measurements of 2011 showed a strong correlation between groundwater and movement, piezometric monitoring was deemed necessary. During the execution of the geognostic surveys, in fact, the position of the aquifer was measured inside holes S1, S2, and S3. In addition, to allow monitoring of changes in the groundwater level with time, a piezoresistive sensor was installed in S2. The results underlined that the piezometric level oscillated between 19 and 8 m under the ground surface. The rains generated a very rapid rise in the water table and the appearance of a number of temporary springs on the slope surface. Moreover, it has also been observed that the elevation of the aquifer in correspondence with intense meteoric events is sudden, following the peak of precipitation with a delay of only a few hours. Even the discharge of water is not excessively prolonged over time, completing itself in a couple of days after the event and
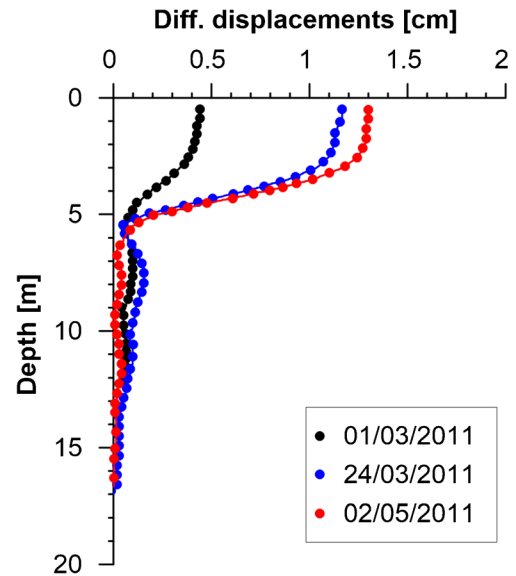

Fig. 5 Inclinometer surveys in CK2 (S3) location (reference date 26/01/2011)

evidencing a relatively high permeability of the slope mass. For instance, in 13–17 March 2011, a cumulative rainfall of 231 mm, with a peak of 141 mm on 16 March, occurred and the piezometer installed in S2 showed the water table rising 3 m in some hours, with a trend of a delay of some hours in relation to the rain's intensity. After the event, the water level returned to the normal level within 2–3 days.

The application of the observational method requires the definition of acceptable limits of slope behavior; for this purpose, the results of a monitoring of surface displacements performed with the SAR technique in the period 1995–2004, i.e., before the landslide occurrence, are considered to establish as an acceptable movement threshold. The stabilization works aimed to reduce the observed deformation under this limit. A maximum strain rate of 3–5 mm/year was considered acceptable as a reference value (Tessari 2014).

Stabilization works

The first proposal of stabilization works focused on the hydraulic control of the slope. For this purpose, a regularization of meteoric water in the upstream side of the road was planned coupled with a large diameter draining well that had to be constructed in the middle between S5 and D positions in the map of Fig. 7. The draining well aimed also to become a mechanical reinforcement of the slope. However, this design hypothesis turned out to be very expensive in light of the results of the geognostic survey carried out subsequently (2011–2012) and not practicable in relation to the limited financial resources of the public agencies.

Consequently, it was decided to substitute the drainage well with a mechanically reinforcing system made up of floating composite anchors. Given the complexity of the local geology and the uncertainties affecting the slope stability, this solution allowed the work to be carried out in successive stages, applying the observational method. The intervention may also be integrated in progress with further anchors if subsequently it were to prove insufficient.

Table 1 Soil parameters for FEM analyses

Material	E [MPa]	φ [°]	c [kPa]
Bellerophon limestone	20	23	5
Val Gardena sandstone	500	36	100
Phyllites	20,000	55	100
Interface	15	33	0.01
	E [MPa]	ε_{el}	H [MPa]
Anchors	200,000	0.43%	1321

E Young modulus, φ friction angle, c cohesion, ε_{el} limit elastic range, H plastic modulus

From June to December 2014, a first group of 32 reinforcements were set up (Fig. 6 and Fig. 7). They are composite anchors, 40–50 m long, formed by a hollow bar with an external diameter of 76 mm, and coupled with 7×0.6" pre-tensioned tendons cemented inside. The pre-tension is limited to 250 kN per anchor to obtain the partially active configuration previously described. Thanks to the presence of inner tendons, the composite anchors have a nominal tensile strength increased from 1100 to 2920 kN (each tendon adds 260 kN of additional resistance), with an increment of cost less than 20% with respect to the self-drilling bar alone. At the head of each anchor, to retain and contrast the slope thrust, a prefabricated reinforced concrete slab, of frustoconical shape and with an outer diameter of 1.5 m, was connected (Fig. 6). The reinforcements were arranged on three single row alignments with a horizontal spacing of 5 m: a first alignment in the Northern portion of the landslide (alignment B), below the road, and two series in the Southern portion (alignment B and C), downstream of the houses (Fig. 7).

For a complete stabilization of the slope and the achievement of an adequate safety factor, the design required the realization of about another 20 anchors, i.e., two more alignments of floating anchors, but in that period, the public agency did not have the entire budget for installing all the anchors needed. It was decided to set up only part of the necessary reinforcement and carefully monitor slope movement with the aim of investigating the effect of the stabilization works realized in terms of displacement rate reduction. In addition, an FE model was created to evaluate the site conditions in the presence of the first intervention and how these conditions could be improved with a second hypothesized intervention.

Post-intervention situation

A new survey with two further inclinometers was activated in March 2015 in correspondence with holes B and D (Fig. 7); even S1, S2, and S3 locations were then recovered for monitoring from October 2016. All the measurements were repeated every few months, until October 2019.

The differential displacements of inclinometers B and D are reported in Fig. 8. Inclinometer B showed significant movements at about 15–16 m of depth; the mean displacement rate is around 4 mm/year, with maximum values that reached 7 mm/year. Similar results were obtained for inclinometer D: the movements are localized at a depth of 15–16 m and the mean velocity is close to 4 mm/year. It is interesting to underline that the position of the sliding surface is located at the interface between the Val Gardena sandstones and the Bellerophon limestones, consistent with the previous hypothesis.

The comparison between the measurements collected before and after the intervention carried out allows the application of the observational method, aimed at evaluating the effect of the anchors and the actual slope stability state. In 2011, the CK2 inclinometer recorded an average displacement rate close to 40 mm/year. Thanks to the intervention made, this rate was reduced by ten times, until 4 mm/year, really close to the chosen threshold of 3–5 mm/year. This is a very good result in terms of stability improvement, but this result underlines that the slope is still moving. Consequently, the current state suggests that to have more complete stabilization of the slope, what is needed is to complete the designed intervention or at least to install other reinforcements.

Concerning the piezometric survey, two holes (probes A and C, Fig. 7) were instrumented in April 2015 with continuous reading piezometers. The devices were placed at − 16.8 m (probe A) and −16.3 m (probe C) from the ground level. In both positions, the piezometric level oscillates between − 15 and − 10 m. The maximum groundwater level was recorded in conjunction with the abundant rains that fell in February 2016 (474 mm), which caused the groundwater level to rise up to a depth of around 8 m.

Unfortunately, in April 2017, the continuous piezometers (Fig. 9) started to show interruptions in data recording. Consequently, the decision was made to adopt some manual measurements of the piezometric level, partially losing in this way the measurement system reliability.

Figure 9 shows that the water level at location C is generally 1–2 m deeper with respect to location A, but the water table oscillations in both the holes range around 5 m, underlining a strong correlation with the precipitation. These recent measures confirmed what was already observed in 2010. The instability in the Cischele landslide can be defined as a slow translational movement, strongly dependent on the interstitial pressures inside the instable body. The occurrence of heavy precipitations suddenly increases the water level, thus increasing the pore pressure, decreasing the shear soil resistance, and causing an acceleration of the slope displacements.

These data indicate that the landslide is partially arrested but not completely stabilized. Moreover, some in-progress damage is evident on the building close to the northern border of the unstable slope. Consequently, the public agency is now planning a supplementary installation of anchors, and in order to help the choice of the optimal anchor configuration, a 3D finite element model of the slope is realized in advance.

Numerical analyses with FE model

Geometry and soil properties

The 3D finite element model is constructed using Midas GTS NX 2019 v1.2. The geometry of the slope (Fig. 10) is created on the base of information collected from three survey campaigns carried out in the years 2011, 2012, and 2014 and from the execution reports of the tie rods, as well as the topographic surveys of the area.

All the volumetric elements in the model (ground, buildings, anchors plates) are simulated using bricks, while anchors are modeled using 1-D embedded truss. The embedded truss does not require node sharing, thus simplifying the model creation. The mother element is determined as the element that includes each embedded truss element node within itself, and the multipoint constraint is used to automatically constrain the nodal displacement of the embedded truss element to be the same as the internal displacement of the mother element (MIDAS GTS-NX User Manual 2019).

The following material models are adopted:

- Soils: isotropic elasto-plastic model according to Mohr-Coulomb criterion;

Fig. 6 Installation of composite anchors at Cischele landslide (2014): (**a**) Bar and strands already infixed; (**b**) external concrete plates of alignment B, visible at the ground surface near the house and below the road

- Buildings and plates: isotropic-elastic model;
- Anchors: elasto-plastic model.

To define the geotechnical parameters of the soils involved in the numerical simulation, a back-analysis was firstly performed, establishing that the configuration identified by a piezometric surface placed at −5 m from the ground level is the most representative of the instability conditions (safety factor FS = 1). The continuous piezometric survey performed after the landslide occurrence indicated a peak of the water table close to −8 m, but this value may not be the maximum value which induced the movements. Considering that the instability occurred during an exceptional rainy event with a returning time of 80 years, it has been prudentially hypothesized that the achievement of the trigger condition is associated with an aquifer reaching a depth of 5 m.

Moreover, a sensitivity study of the effect on the model results of a soil parameters variation was realized. For the model thus assumed, the results of these analyses highlighted how even important variations in the resistance parameters of the deepest layers do not significantly affect the FS value. The same happens for the interface layer where a 13° decrease in the friction angle value determines an FS variation of less than 3%. Unlike what happens for the Bellerophon limestones, whose friction angle strongly affects FS, as shown in Fig. 11. These results support the hypothesis that the most likely sliding surface of the landslide can extend mainly within the limestone layer.

The geotechnical parameters, which in the sensitivity analysis determine the collapse condition of the slope (FS=1), are listed in Table 1.
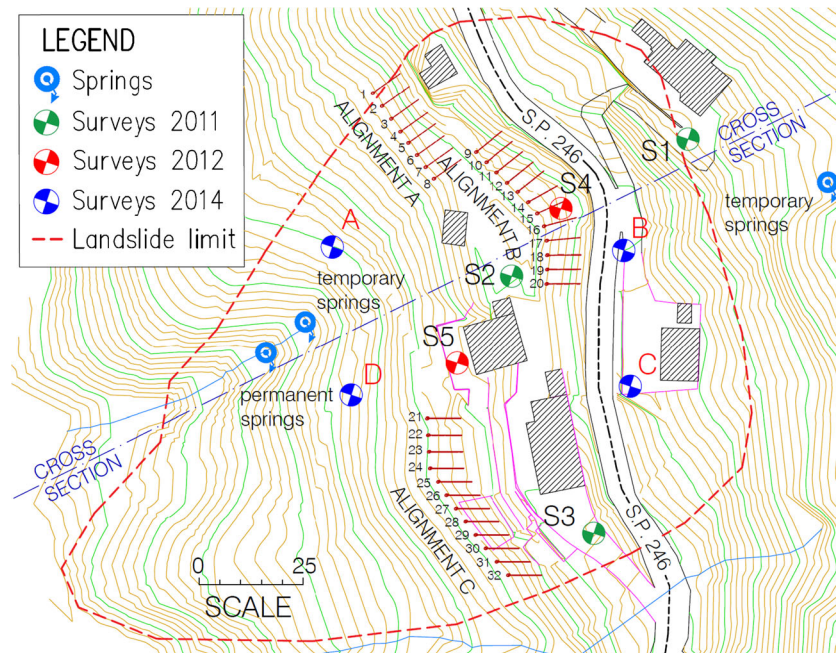

Fig. 7 Cischele landslide map, with indication of the positions of the realized anchors
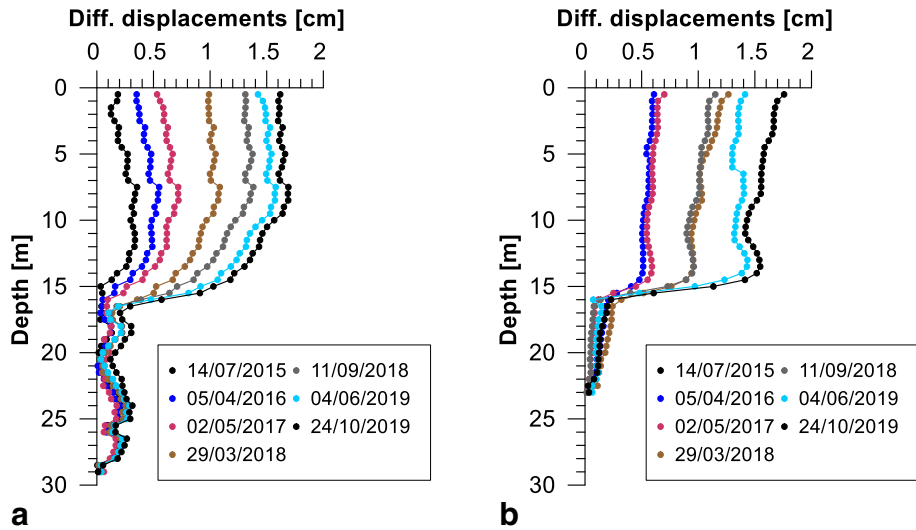
Fig. 8 Inclinometer surveys at locations: (**a**) B; (**b**) D (refernce date 10/03/2015)

Analysis and outputs

In order to determine the instability effects and the stresses acting on the tie rods, after the calibration of the geotechnical parameters of the materials involved, two types of analysis were performed:

- Non-linear static analysis of water level rising (*NLS-WLR*): this analysis studies the displacement of the slope induced by the rising of the ground water level consequent to a rainfall. To this aim, the model is initialized by considering a water level at about −22 m from the surface, and after having nullified the displacements and the strain of the initialization phase, the analysis simulates the rising of the WT to a higher position. In particular, WT at −20 m, −15 m, −12.5 m, −10 m, −7.5 m, and−5 m from ground level (GL) have been considered. The analysis takes into account the non-linear behavior of the soil and permits the evaluation of the axial forces activated in the reinforcements resulting from the WT rise, reproducing what generally happens in a slope reinforced with passive anchors. The pore pressure in the stress analysis is included in steady state condition, thus considering a drained behavior of the

different soils; the variation of the WT position therefore modifies the distribution of the effective stresses in the different soil layers.

- Stability analysis by strength reduction method (SRM): it is a non-linear analysis in which, starting from a stable geometry, the soil shear strength parameters (ϕ' and c') are progressively reduced until a collapse condition is reached. Numerically, this condition occurs when it is no longer possible to obtain a converged solution. The analysis is fairly equivalent to a stability analysis performed with limit equilibrium methods (Griffiths and Lane 1999; Matsui and San 1992; MIDAS GTS-NX User Manual 2019) and permits to evaluate the slope global safety factor as the factor by which the soil strength needs to be reduced to reach failure. This analysis is repeated for every WT level, in order to understand the safety reserve corresponding to the various hydraulic conditions.

Three different intervention situations are investigated, as indicated in Fig. 12:
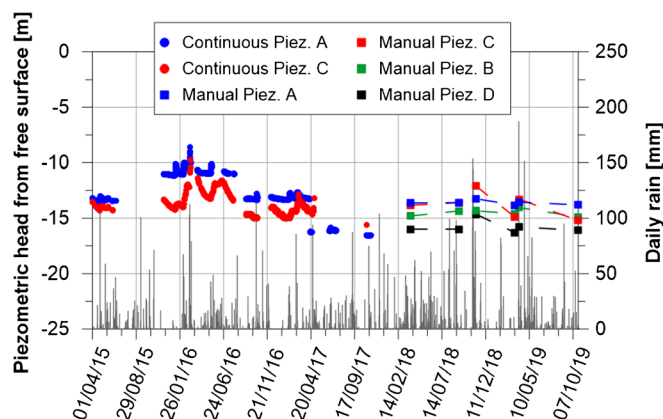

Fig. 9 Piezometer surveys at A, C, B, and D locations

Section G-G

Bellerophon limestones | Val Gardena sandstones
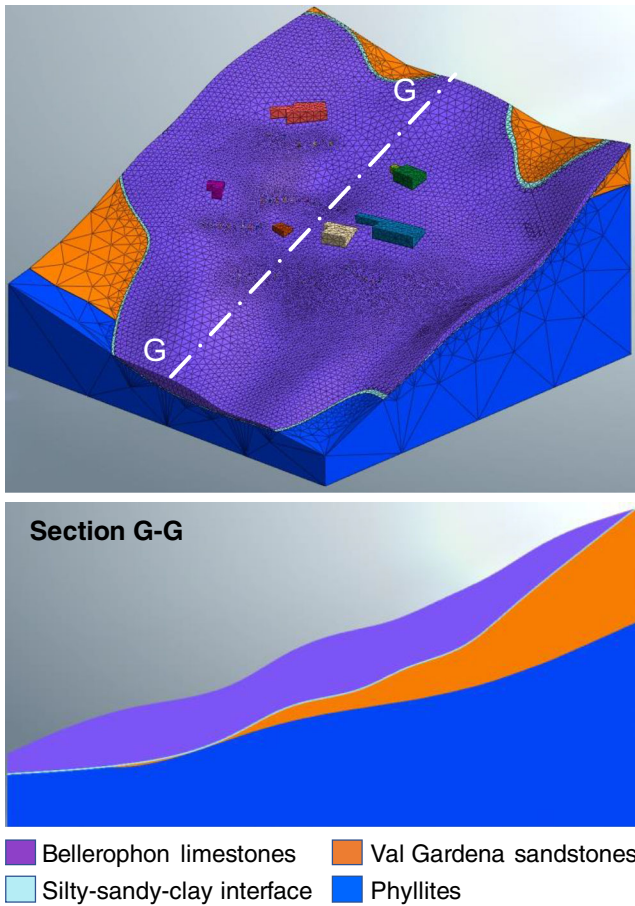Silty-sandy-clay interface | Phyllites

Fig. 10 FEM model geometry and mesh

- without any intervention (case 1);
- with the anchors already realized (case 2);
- with a hypothetical second group of anchors added to the 1° group already realized (case 3).

The first group of reinforcements are those realized in 2014, e.g., the 32 anchors arranged in three alignments (A, B, and C), while the hypothetical second group of 15 tie rods (not realized) is
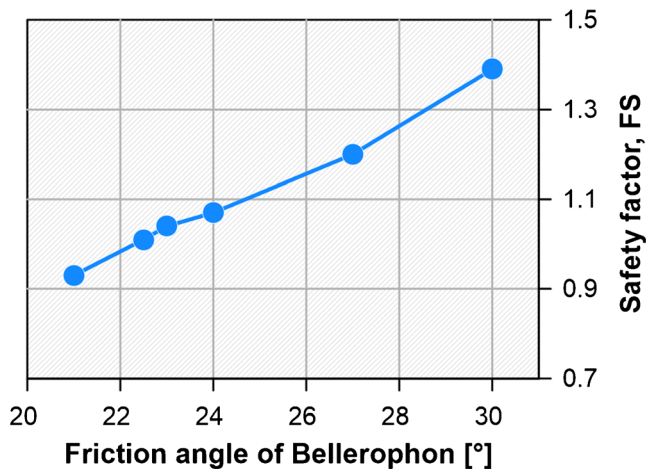
Fig. 11 Effect of the limestone friction angle on FS

considered distributed along two lines (alignments D and E). The quantity and numbering of anchors in each alignment are:

- Alignment A: no. 8 anchors (from 1 to 8);
- Alignment B: no. 12 anchors (from 9 to 20);
- Alignment C: no. 12 anchors (from 21 to 32);
- Alignment D: no. 10 anchors (from 33 to 42);
- Alignment E: no. 5 anchors (from 43 to 47).

In finite element analysis, the problem of the mesh size definition is well known (e.g., More and Bindu 2015; Li and Wierzbicki 2009). The accuracy of the results and the required computing time are in fact strongly dependent on the finite element size. The FE models with fine mesh yield highly accurate results but may take longer computing time. On the other hand, those FE models with coarse mesh may lead to less accurate results but smaller computing time. To consider this aspect, three different mesh configurations were firstly realized, counting 307,004, 844,908, and 1,998,016 nodes, respectively. Each simulation included both an NLS analysis with an assigned groundwater level (−10 m) and a stability analysis obtained by SRM; in this way, the time needed to complete this analysis provides an important reference for estimating the overall time to perform 6 water table positions for each of the three cases analyzed. In agreement with what already evidenced by the authors, the coarser mesh leaded to underestimating the deformations and consequent displacements, thus overestimating the safety factor of the slope. On the other hand, the finer mesh requested more than 52 h to complete only one WT position analysis. This means that an estimate of the computing time required to perform all the simulations would exceed 40 days, thus making this choice of mesh size impractical. The intermediate case instead allowed to obtain a good
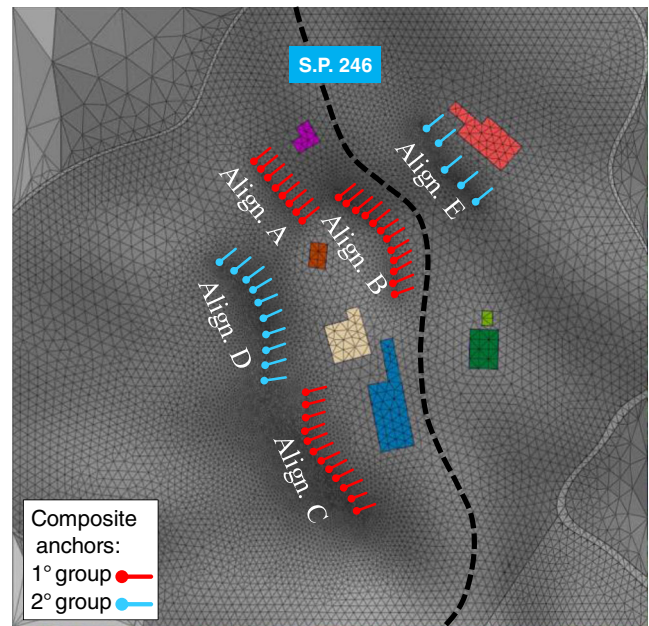

Fig. 12 FEM model geometry and mesh with positions of the two groups of anchors

compromise between reliability of the results and computational times (around 8 h for one WT position, nearly 5 days for all the cases). It should be emphasized that all the analyses presented in the follow allow for a relative comparison, not aiming to be an absolute reference for the case study. Furthermore, the calibration phase for selecting the soil parameters was carried out with the back-analysis (FS=1 for WT −5 m) using the medium mesh: the same mesh was then adopted for all the other analyses.

Numerical analysis results

The critical values of the strength reduction factor (SRF) obtained with the various water levels with the SRM analysis, and assumed here as the safety factor FS, are listed in Table 2. In Figs. 13 and 14 are reported for comparison the total displacement distribution obtained with the NLS-WLR analyses for a WT at −7.5 m from GL with the three cases of absence of reinforcements or with 3 or 5 alignments.

It is possible to note that without interventions, the slope becomes unstable when the water table rises to −5 m of depth, according with the calibration previously performed. Indeed, significant deformations were observed when the water table reached the minimum in situ observed depth, around 7–8 m from the ground surface (Fig. 13).

Of course, the anchors show stabilization effects, as FS increases for all the water levels considered. For instance, the anchors already realized (case 2) permit the increase of the FS value corresponding to a water table at −10 m from 1.06 to 1.20, which corresponds to an increment of 10%. When the water table reaches −5 m, the slope still proves to be stable (FS = 1.03), but the value of FS is so close to the unit that it indicates a condition approaching instability. The new group of anchors (case 3) would make it possible to further increase the safety factor, reaching a more stable condition for every water table position examined. Anyway, the value of safety factor when the water table is at −5 m is still not completely satisfactory, even if it becomes 1.10. Nonetheless, considering that the peak value observed for the water table was close to −7.5 m, it is evident that the realization of the further alignment of anchors would give a relevant stabilization effect, increasing FS from 1.10 to 1.14.

The maximum movement observed in the original slope when the WT arrives to −7.5 m exceeds 40 cm (Fig. 13). The zone of maximum displacement is located immediately downstream of the road S.P. 246 in the central part of the slope. Moreover, the distribution of displacements shows important variability in space, justifying the large fissures observed on site. The displacements corresponding to the same WT for case 2 and case 3 are reported

in Fig. 14 using an enlarged color scale respect that is used in Fig. 13 to better visualize the space distribution of displacements, which are strongly reduced. In fact, by the comparison of analyses with the same water conditions, it is evident that the entity of displacements significantly reduces with the anchor installation and moving from case 2 to case 3, reaching maximum values of less than 22 cm and 17 cm, respectively.

Of course, with a lower WT, the displacements are smaller; for example, when the water table is located at −10 m from the ground level, the maximum displacement moves from 10.2 cm with no reinforcements to 6.1 cm with the first group of anchors and to 5.4 cm with the second group.

Figure 14b and d also show the distribution of displacements along section B–D connecting the positions of inclinometers B and D, again for the case with WT at −7.5 m. Moreover, in Fig. 14b, the vertical distribution of displacements obtained at the inclinometers B and D after the anchor installation are overdrawn for comparison. It is evident that the model correctly identifies the sliding surface; moreover, it is interesting to note that the reinforcements of the hypothetic alignments D and E would reduce slope instability, particularly in the part of the slope above the road.

Stress and strain on anchors

For all the phases and the geometric configurations previously presented, the stresses acting on the reinforcements were analyzed. For the anchors, an elasto-plastic constitutive law, like that sketched in Fig. 15, was adopted to numerically describe the axial stress-strain behavior of the anchors.

The distribution of the axial forces along the anchors follows, in all cases, a pattern similar to those shown in Fig. 16; the stress is minimal in correspondence with the anchor plates and increases with depth in the "active" portion of the reinforcement (inside the moving mass). The maximum traction value is observed near the interface with the more rigid layer, represented by the sandstones, where the lateral shear stresses reverse the direction and the "passive" portion of the tie rod begins. In particular, Fig. 16 shows the axial forces along anchor no. 14 for two different water table levels and, respectively, for the situation with only the first group of reinforcements installed (case 2, Fig. 16a and b) and when both the groups are included (case 3, Fig. 16c and d). This anchor is located in the central portion of alignment B, exactly in the center of the instable body. Comparing Fig. 16a and 16b, it is evident that when the water table level moves from −12.5 to−7.5 m under the ground surface, the maximum axial force passes from 1917 to 2500 kN in case 2. The increase in the axial force is slightly reduced when all five anchor alignments are present: in this case, as Fig. 16d shows, the axial force of anchor no. 14 reaches the maximum value of 2478 kN. A less significant difference for the anchor axial force is observed between case 2 and case 3 when the water table is at −10 m or deeper. On the contrary, the effect of the floating anchors of alignments D and E becomes relevant when the instable mass begins to show increasing displacements.

It is very interesting to compare the maximum axial forces of anchors, T_{max}, as they are calculated from the NLS-WLR analyses in relation to their position, the water level, and the anchor configurations (Figs. 17 and 18). In general, the maximum axial forces tend to increase with the increasing water table, and in particular, the reinforcements suffer an important increase of T_{max}

Table 2 Safety factors obtained in the different cases from the FEM analyses.

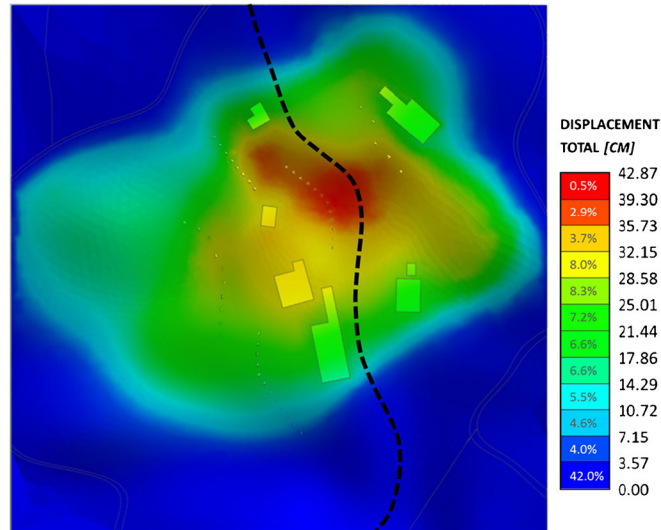| Water table position (m)	Safety factor, FS		
	Case 1	Case 2	Case 3
−20	1.19	1.30	1.35
−15	1.18	1.27	1.30
−12.5	1.17	1.25	1.29
−10	1.12	1.20	1.25
−7.5	1.06	1.10	1.14
−5	less than 1	1.03	1.10

Fig. 13 Contour plot of the total displacements for case 1 in NLS-WLR analysis conditions, imposing WT =−7.5 m

when the WT reaches or exceeds the level of −10 m from the ground level. Figure 17 shows that the anchors reach the ultimate tensile strength (2920 kN) when the water table is at −5 m from the slope level. This is evident for the anchors of alignment B, located
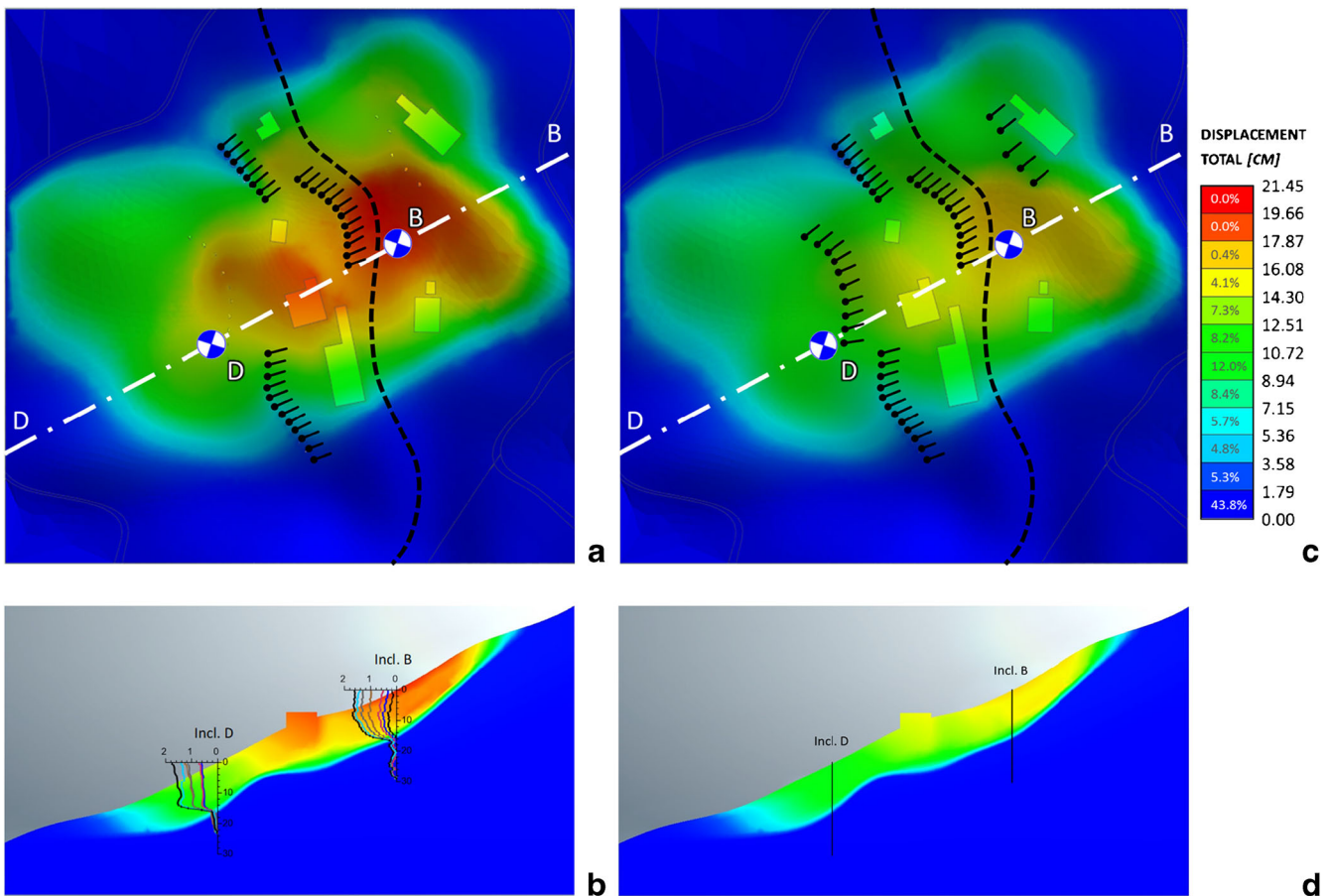

Fig. 14 Contour plot of the total displacements in NLS-WLR analysis conditions, imposing WT =−7.5 m for (**a**) map view and (**b**) section B–D case 2; and (**c**) map view and (**d**) section B–D case 3. The contour range is different from that of Fig. 13
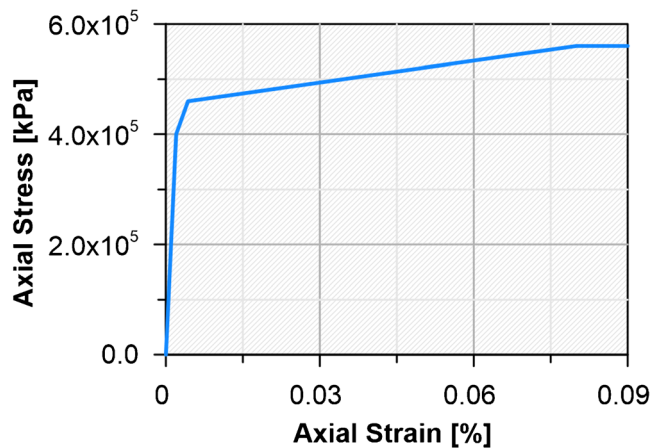
Fig. 15 Anchor's constitutive law

in the central portion of the landslide, while the more external reinforcements of alignments A and C still present a reserve of resistance, even if not very high.

The addition of two lines of tie rods (alignment D and E) leads to a general reduction of the axial force and to a more homogeneous distribution of the stresses in the three alignments of the first group of reinforcements. This reduction is particularly evident when the water table is located at −5 m from GL, while it is less significant when the water table drops below 10 m of depth. Moreover, the anchors of the 2nd group, arranged in two lines upstream and downstream of alignment B, respectively, are subjected to greater axial stresses than the reinforcements of the 1st group; this suggests that the position of these two alignments is correctly hypothesized.

As already observed, some anchors reach the ultimate tensile strength when the water table rises to −5 m, in particular, all the anchors of alignment B in case 2, and all those of alignments D and E in case 3. Figure 19a shows the axial force profile along anchor no. 14 in case 2, while Fig. 19b and 19c report the axial forces in anchors no. 36 and no. 45, in case 3. Note that all the plots are for WT at −5 from GL and that all the anchors reported here are close to the central section of the landslide, in alignments B, D, and E, respectively. It is observable that all these anchors reach the maximum axial force at the intersection with the interface, the layer in which the sliding occurs. Consequently, the anchor, reaching its ultimate limit, shows precisely the depth at which it encounters the interface, corresponding to the position where the axial force is the maximum. Clearly, this intersection takes place at different depths, depending on the position and inclination of each anchor: anchor no. 14 shows the peak around 20 m far from the external slab, while anchors no. 36 and no. 44 around 25 m and 13 m, respectively.

Once this limit is reached, the axial force inside the reinforcement cannot increase anymore. The consequent effect is a redistribution of the axial load along the length of the same anchor with a gradual increase of the anchor tension in a decreasing distribution moving from the peak towards the external end. The portion of anchors in the passive zone does not show evident variations, once the anchor has reached the ultimate limit. Moreover, if the pull-out resistance of the rock in the passive zone is very good, a portion of the anchors resulted unloaded. This behavior suggests that the anchorage has gradually more and more points in limit conditions in the active zone, while no great variations occur within the part included in the passive zone, a part that can therefore be reduced installing a shorter anchorage. In fact, it is evident that all the anchors shown in Fig. 19 have an oversized length, while they show acceptable behavior in terms of resistant strength, taking into account that the water table has never arrived at a level close to −5 m.
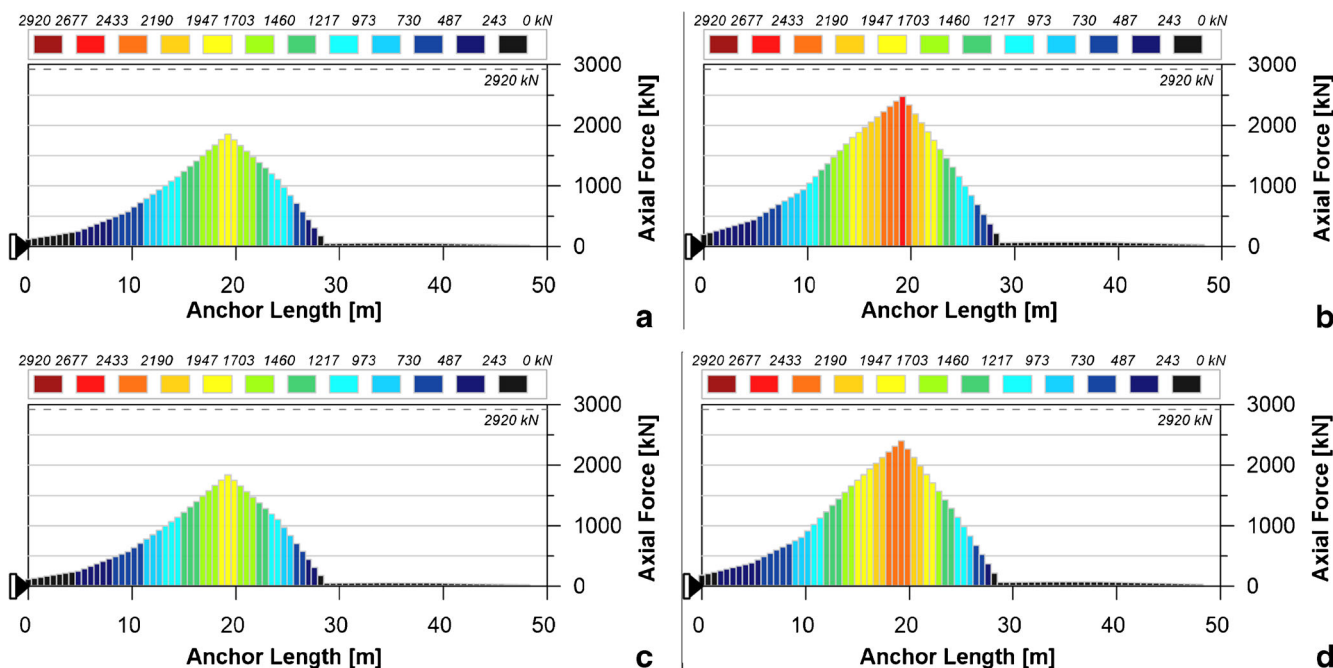

Fig. 16 Axial forces and bond stresses of anchor 14: (**a**) W.T. −12.5 m and (**b**) W.T. −7.5 m − case 2; (**c**) W.T. −12.5 and (**d**) W.T. −7.5 m − case 3
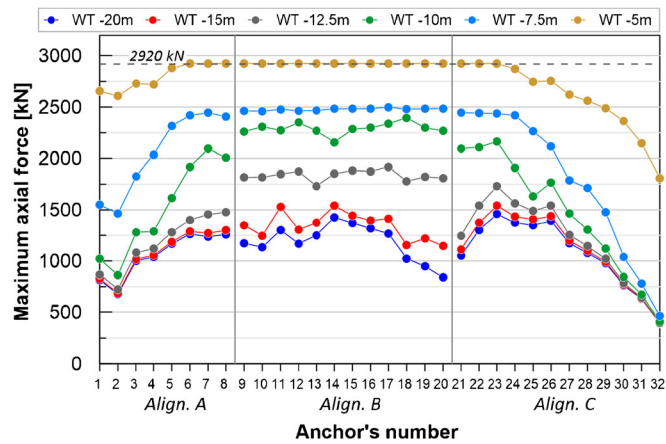
Fig. 17 Maximum axial forces on various anchors for different position of water table in case 2

Conclusions

The paper presents an interesting modular stabilization of a landslide with composite floating anchors, a new type of passive reinforcements obtained by introducing a small modification to the standard bars for soil nailing; in this way, it is possible to combine the advantages of self-drilling bar installation with that of traditional anchors.

Among their advantages, the most important are the very flexible installation, the high tensile resistance, the modularity, and, above all, the adaption of actions in relation to eventual displacements successively experienced by the slope, if the latter has not completely stabilized. Moreover, they offer the possibility to be partially pre-tensioned in order to reduce the displacements needed to come in effect.

The modularity, combined with the observational approach currently included in by many national codes, allows the stabilization of slow landslides in compliance with cost constraints. In fact, when the economical budget is limited, a first minor intervention can be performed immediately after the landslide occurs; this can be subsequently improved to increase the degree of safety of the area, according to the results of a monitoring system and to an accurate analysis of the slope stability conditions. The choice of the threshold value of the maximum acceptable displacement rate for a slope allows to design the type of intervention and, therefore,

to accurately verify its effectiveness. The modularity of the installation of the reinforcements then allows the intervention to be adapted to the real stratigraphy and consistency of the in situ formation found during the construction of the work. In addition, after the end of the work, if the slope has not actually decreased its deformation rate below the chosen limit value, an addition of reinforcements can be installed. In conclusion, the use of modular and adaptable reinforcements makes it possible to create site-specific solutions, thus limiting costs and optimizing performance.

To make the most of these advantages, it is fundamental to activate a monitoring system, and, in the meanwhile, perform some analyses. To this aim, the availability of 3D FE models of the slope and anchors now permits a better exploitation of the advantages of composite anchors, analyzing their optimal spatial distribution on the slope.

In the case study presented, although the number of reinforcements installed in a first phase does not allow complete elimination of post-intervention slope deformations, the measurements performed for 4 years after the anchors' installation show a significant reduction of the post-work displacement rates, thus proving the viability and technical efficiency of the method. In the current state, there are two areas not yet fully stabilized. Here, the 3D FE model shows that important displacements could still
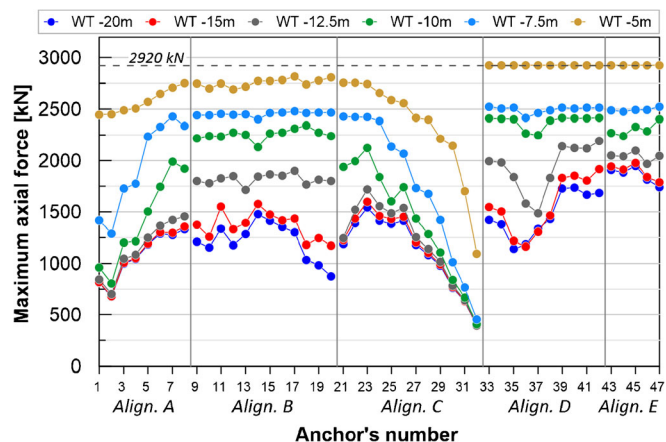

Fig. 18 Maximum axial forces on various anchors for different position of water table in case 3
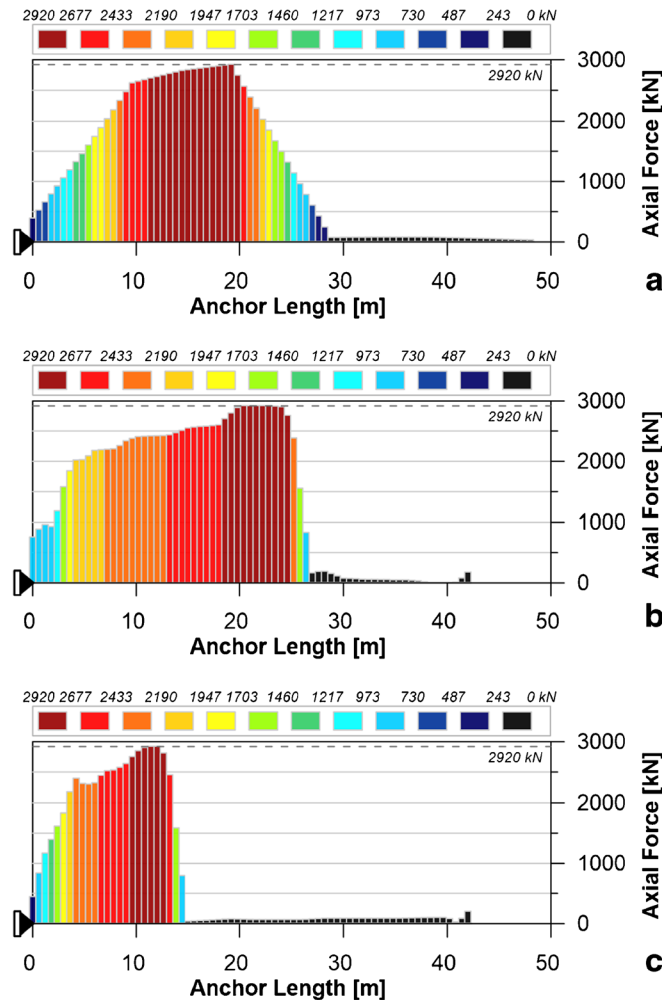
Fig. 19 Axial forces: (**a**) anchor nr 14, W.T. −5 m – case 2; (**b**) anchor nr 36, W.T. −5 m – case 3; (**c**) anchor nr 45, W.T. −5 – case 3

occur if particularly heavy rains, such as those which triggered the initial movements, cause significant increases in the piezometric level. A second intervention phase has been hypothesized, with the aim of further reducing the expected deformations in the areas at the highest risk of instability and redistributing the actions stressing the most active reinforcements. The additional anchors allow reduction of the maximum tractions in the bars by 10–20% in normal conditions, even if when the water table reaches the maximum level supposed many anchors still work at their limits.

References

Abramson LW, Lee TS, Sharma S, Boyce GM (2002) Slope stability and stabilization methods. 2nd. USA: Wiley. ISBN: 978-0-471-38493-9

Ansari N, Domitric C (1992) Soil Nailing earth shoring system - a ten year update, Isherwood Associates

Baecher GB, Christian JT (2008) Spatial variability and geotechnical reliability, Reliability-Based Design in Geotechnical Engineering, K.K. Phoon (Ed.), Taylor & Francis, 76-133

Bisson A (2015) Sirive® floating anchor for landslide stabilization. PhD thesis at University of Padova. (In Italian)

Bisson A, Cola S (2014) Ancoraggi flottanti per la stabilizzazione di movimenti franosi lenti. XXV Convegno Nazionale di Geotecnica AGI: La geotecnica nella difesa del territorio e delle infrastrutture dalle calamità naturali, 4-6 giugno, Baveno, Vol. 2, 327-334, Edizioni AGI, ISBN 9788897517054 (In Italian)

Bisson A, Cola S, Tessari G, Floris M (2015) Floating anchors in landslide stabilization: the Cortiana case in North-Eastern Italy. In Engineering Geology for Society and Territory - Volume 2, 2083-2087. Springer, Cham. https://doi.org/10.1007/978-3-319-09057-3_372

Bisson A, Cola S, Carollo I (2016) Ancoraggi compositi pretesi: analisi delle sollecitazioni indotte nel terreno. 6° IAGIG: L'ingegneria geotecnica al servizio delle grandi opere: necessità e opportunità, 20-21 Maggio 2016, Verona (Italy), 24-27. (In Italian)

Bisson A, Cola S, Baran P, Zydroń T, Gruchot AT, Murzyn R (2018) Passive composite anchors for landslide stabilization: an Italian-Polish research program. In Landslides and Engineered Slopes. Experience, Theory and Practice: Proceedings of the 12th International Symposium on Landslides (Napoli, Italy, 12-19 June 2016) (p. 433). CRC Press. https://doi.org/10.1201/9781315375007

Bustamante M, Doix B (1985) Une méthode pour le calcul des tirants et des micropieux injectés. Bull Liaison Lab Ponts Chauss, (140)

Calvello M (2017) From the observational method to "observational modelling" of geotechnical engineering boundary value problems. Geotechnical safety and reliability honouring Wilson H. Tang. Geotechnical Special Publication No. 286, ASCE; 2017, 101–117. https://doi.org/10.1061/9780784480731.008

Cheng YM, Lansivaara T, Wei WB (2007) Two-dimensional slope stability analysis by limit equilibrium and strength reduction methods. Comput Geotech 34:137–150. https://doi.org/10.1016/j.compgeo.2006.10.011

Cola S, Schenato L, Brezzi L, Pangop T, Chantal F, Palmieri L, Bisson A (2019) Composite anchors for slope stabilisation: monitoring of their in-situ behaviour with optical fibre. Geosciences 9(5):240. https://doi.org/10.3390/geosciences9050240

Dawson EM, Roth WH, Drescher A (1999) Slope stability analysis by strength reduction. Géotechnique 49(6):835–840. https://doi.org/10.1680/geot.1999.49.6.835

EN 14490:2010 (2010) Execution of special geotechnical works — soil nailing

Eurocode 7: BS EN 1997–1–2004 (2004) Geotechnical design–Part I: General Rules

FHWA-IF-03-017 (2003) Geotechnical Engineering circular No. 7 – Soil Nail Walls

Floris M, D'Alpaos A, De Agostini A, Tessari G, Stevan G, Genevois R (2013) Variation in the occurrence of rainfall events triggering landslides. In: Landslide Science and Practice. Springer, Berlin, Heidelberg, pp 131–138. https://doi.org/10.1007/978-3-642-31337-0_17

Galve JP, Cevasco A, Brandolini P, Piacentini D, Azañón JM, Notti D, Soldati M (2016) Cost-based analysis of mitigation measures for shallow-landslide risk reduction strategies. Eng Geol 213:142–157. https://doi.org/10.1016/j.enggeo.2016.09.002

Gao YF, Zhang F, Lei GH, Li DY (2013) An extended limit analysis of three-dimensional slope stability. Géotechnique 63(6):518–524. https://doi.org/10.1680/geot.12.T.004

Gassler G, Gudehus G (1981) Soil nailing – some aspects of a new technique. Proc. 10th ICSMFE, Stockholm, Vol. 3, 665.670

Geoguide7 (2008) Guide to soil nail design and construction. Geotechnical Engineering Office, Hong Kong

Griffiths DV, Lane PA (1999) Slope stability analysis by finite elements. Geotechnique 49(3):387–403. https://doi.org/10.1680/geot.1999.49.3.387

Heymann G, Rohde AW, Schwartz K, Friedlaender E (1992) Soil nail pull-out resistance in residual soils. IS on Earth Reinforcement Practice, Fukuoka, Kyushu, 487–492

Hicks MA, Spencer WA (2010) Influence of heterogeneity on the reliability and failure of a long 3D slope. Comput Geotech 37:948–955. https://doi.org/10.1016/j.compgeo.2010.08.001

Hong HP, Roh G (2008) Reliability evaluation of earth slopes. JGGE 134(12):1700–1705. https://doi.org/10.1061/(ASCE)1090-0241(2008)134:12(1700)

Ji J, Zhang C, Gao Y, Kodikara J (2018) Effect of 2D spatial variability on slope reliability: a simplified FORM analysis. Geosci Front 9:1631–1638. https://doi.org/10.1016/j.gsf.2017.08.004

Kazmi D, Qasim S, Harahap ISH, Baharom S, Mehmood M, Siddiqui FI, Imran M (2017) Slope remediation techniques and overview of landslide risk management. Civ Eng J 3(3):180–189. https://doi.org/10.28991/cej-2017-00000084

Li Y, Wierzbicki T (2009) Mesh-size effect study of ductile fracture by non-local approach. Proceedings of the SEM Annual Conference, June 1-4, 2009, Albuquerque New Mexico USA

Matsui T, San KC (1992) Finite element slope stability analysis by shear strength reduction technique. Soils Found 32(1):59–70. https://doi.org/10.3208/sandf1972.32.59

MIDAS GTS-NX User Manual (2019)

More ST, Bindu RS (2015) Effect of mesh size on finite element analysis of plate structure. Int J Eng Sci Innov Technol 4(3):181–185

Morgenstern NR (1992) The evaluation of slope stability – a 25 year perspective, stability and performance of slopes and embankments – II, Geotechnical Special Publication No. 31, ASCE; 1992

Ng AFH, Lau TMF, Shum LKW, Cheung RWM (2007) Review of selected landslides involving soil-nailed slopes. Geotechnical Engineering Office, Hong Kong, Landslide Study Report, LSR, 8, 2007

Norme tecniche per le costruzioni - NTC (2018) Ministero delle infrastrutture e dei trasporti (in Italian). Gazzetta Ufficiale, Decreto Ministeriale 17 gennaio 2018

Peck RB (1969) Advantages and limitations of the observational method in applied soil mechanics. Geotechnique 19(2):171–187. https://doi.org/10.1680/geot.1969.19.2.171

Popescu ME (2001) A suggested method for reporting landslide remedial measures. Bull Eng Geol Environ 60:69–74. https://doi.org/10.1007/s100640000084

Popescu ME (2002) Landslide causal factors and landslide remedial options, keynote lecture. In: Proc. of the 3rd IC on Landslides, Slope Stability and Safety of Infra-Structures, Singapore, 61–81

Popescu ME, Seve G (2001) Landslide remediation options after the international decade for natural disaster reduction (1990 - 2000), Keynote Lecture, Proc. Conf. Transition from Slide to Flow - Mechanisms and Remedial Measures, ISSMGE TC-11, Trabzon, 73-102

Pun WK, Urciuoli G (2008) Soil nailing and subsurface drainage for slope stabilization. In Landslides and Engineered Slopes. From the Past to the Future, Two Volumes+ CD-ROM (pp. 107-148). CRC Press

Sharma M, Samanta M, Sarkar S (2019) Soil nailing: an effective slope stabilization technique. In: Landslides: Theory, Practice and Modelling. Springer, Cham, pp 173–199. https://doi.org/10.1007/978-3-319-77377-3_9

Stark TD, Hussain M (2012) Empirical correlations: drained shear strength for slope stability analyses. JGGE 139(6):853–862. https://doi.org/10.1061/(ASCE)GT.1943-5606.0000824

Stocker M (1976) Bodenvernagelung, Vorträge der Baugrundtagung, Nürnberg, Deitsche Gesellschaft für Erd- und Grundbau e.v., Essen

Tessari G (2014) Caratterizzazione e modellazione di fenomeni geologici di instabilità attraverso tecniche di telerilevamento satellitare e simulazioni numeriche. PhD thesis at University of Padova. (In Italian)

Turner JP, Jensen WG (2005) Landslide stabilization using soil nail and mechanically stabilized earth walls: case study. JGGE 131(2):141–150, ASCE. https://doi.org/10.1061/(ASCE)1090-0241(2005)131:2(141)

Ugai K, Leshchinsky D (1995) Three-dimensional limit equilibrium and finite element analysis: a comparison of results. Soils Found 35(4):1–7. https://doi.org/10.3208/sandf.35.4_1

Yin JH, Su L-J, Cheung RWM, Shiu Y-K, Tang C (2009) The influence of grouting pressure on the pullout resistance of soil nails in compacted completely decomposed granite fill. Géotechnique 59(2):103–113. https://doi.org/10.1680/geot.2008.3672

L. Brezzi (✉) · **D. Pasa** · **S. Cola**
Department ICEA,
University of Padova,
via Ognissanti 39, 35129, Padova, Italy
Email: lorenzo.brezzi@unipd.it

A. Bisson
Sirive S.r.l.,
via A. Fogazzaro 71, 36073, Cornedo Vicentino (VI), Italy